Liquid Crystals

Publication details, including instructions for authors and subscription information:
http://www.informaworld.com/smpp/title~content=t713926090

U-Shaped dimeric liquid crystals derived from phthalic acid

G. S. Attard; A. G. Douglass

To cite this Article Attard, G. S. and Douglass, A. G.(1997) 'U-Shaped dimeric liquid crystals derived from phthalic acid', Liquid Crystals, 22: 3, 349 — 358

To link to this Article: DOI: 10.1080/026782997209423

URL: http://dx.doi.org/10.1080/026782997209423

LIQUID CRYSTALS, 1997, VOL. 22, NO. 3, 349–358

U-Shaped dimeric liquid crystals derived from phthalic acid

by G. S. ATTARD* and A. G. DOUGLASS

Department of Chemistry and Southampton Liquid Crystal Institute,
University of Southampton, Southampton SO17 1BJ, U.K.

(*Received 22 July 1996; in final form 19 October 1996; accepted 31 October 1996*)

Details of the transitional properties of four homologous series of U-shaped liquid crystal materials, the benzene-1,2-di-(4-carboxyalkoxybenzylidene-4′-*n*-alkylanilines), are presented. The spacers incorporate 3 to 6 methylene units, whilst terminal aliphatic chain lengths are varied from 1 to 12 units. Members of the two homologous series with an odd number of methylene units in the spacer form nematic and smectic phases as a function of terminal chain length. Materials with an even number of methylene units in the spacer are purely smectogenic, and in both series the first two homologues form only smectic B phases. For all four series the higher homologues show the phase sequence $S_{F/I}$–S_C–S_A–I. X-ray diffraction studies have shown that these smectic phases are composed of molecules arranged in bilayers.

1. Introduction

As early as 1907 Vorländer proposed his rule that 'the liquid crystalline state is obtained for the most linear of molecules' [1] and indeed a wide variety of rod-like mesogenic molecules have been synthesized. Of course, alternative forms of molecular anisometry have been shown to be conducive to mesophase formation [2]. However, in following the Vorländer rule, a structural unit commonly used in mesogenic cores is a 1,4-disubstituted benzene ring which, if attached to other unsaturated systems, forms an extended semi-rigid unit. The rigidity ensures a high molecular anisometry and a concomitant anisotropy in the polarizability. Disubstitution of the benzene ring in the 1,2- or 1,3-positions results in U-shaped or bent molecules that deviate significantly from the 'ideal' elongated lath-like structure. Consequently very few such systems have been reported to form liquid crystal phases. The first such report was indeed by Vorländer himself in conjunction with Apel [3]. For example compound **1** forms an enantiotropic nematic phase.

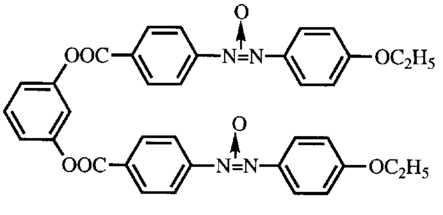

1

The homologous series **2** and **3** provide examples of U-shaped mesogens based on a 1,2-disubstituted benzene ring [4, 5]. The phase behaviour of these series is similar. Both form nematic phases for homologues having $n \leqslant 8$; smectic A phases increase in stability with increasing terminal chain length and the higher homologues are purely smectogenic. A number of these smectogenic materials exhibit smectic B phases. Interestingly, all but one of the nematic–isotropic transition entropies ($\Delta S/R$) are less than 0·14; the weakly first order nature of these transitions is presumably a result of the high molecular biaxality. It has been suggested, on the basis of X-ray diffraction studies, that the molecules are arranged in a partial-bilayer structure in the smectic A phases. Kato *et al.* [6] have used stilbazole derivatives **4**, in conjunction with the diacids **a**, **b**, **c** to form linear, bent, and U-shaped hydrogen bonded mesogenic cores. It was found that the complexes of the 1,3- and 1,4-disubstituted benzene dicarboxylic acids form smectic phases stable up to the decomposition temperatures (≈250°C), whilst the U-shaped 1,2-derivatives form nematic phases that clear below 140°C.

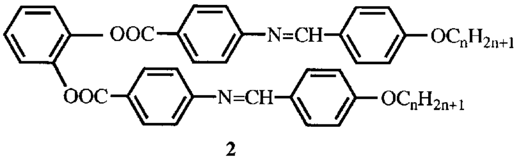

2

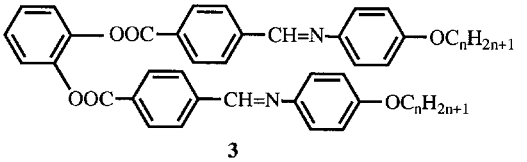

3

---

*Author for correspondence.

0267–8292/97 $12·00 © 1997 Taylor & Francis Ltd.

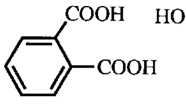

a

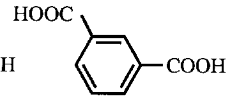

b

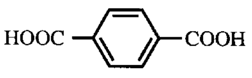

c

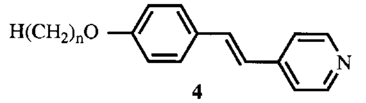

4

The introduction of flexible spacers between mesogenic units can have a profound effect on the liquid crystal properties. The properties of dimeric liquid crystal molecules have been investigated (see for example [7–10]) and some general rules obtained, for example with regard to the strong dependence of mesophase stability on spacer parity. In this paper we describe the phase transition behaviour of U-shaped dimeric materials, (structure **5** in the scheme), having two Schiff's base moieties attached to a 1,2-disubstituted phenyl diester via flexible spacers. In these materials we expect the liquid crystalline polymorphism and phase stability to be related to the parities of the spacer chains since these will determine the relative geometric orientation of the two rod-like moieties.

2. Experimental

The benzene-1,2-di-(4-carboxyalkoxybenzylidene-4′-*n*-alkylanilines) **5** were synthesized by the route outlined in the above scheme. Final products were purified by recrystallisation until the transition temperatures were constant. Intermediates and products were characterized by IR (Perkin-Elmer 1600 series FT-IR), ^{1}H and ^{13}C NMR spectroscopies (JEOL FX90Q FT-NMR and Bruker AM 360 MHz). Randomly selected final products gave satisfactory elemental analyses and mass spectra (VG 70-250 GC-MS).

The synthesis of the benzene-1,2-di-(4-ω-carboxyalkoxybenzylidene-4′-*n*-alkylanilines), **5**, is illustrated for the compound with $n=4$ and $m=7$ (**4,7-*ortho***).

2.1. *Synthesis of 4-ω-bromobutyloxybenzaldehyde*

A mixture of α,ω-dibromobutane (10 eq., 0·4 mol), 4-hydroxybenzaldehyde (1 eq., 0·04 mol) and anhydrous potassium carbonate (7 eq., 0·28 mol) was heated under reflux with stirring for 6 h in dry diethyleneglycol dimethyl ether (DMGE) (80 ml). The hot mixture was filtered and the solid washed with hot absolute ethanol (4 × 50 ml). The ethanol was removed from the liquor on a rotary evaporator, and both the DMGE and the dibromobutane were removed using a short-path distillation apparatus. The product was distilled and purified by column chromatography (30:70, diethyl ether: light petroleum, b.p. 60–80°C). Yield 72%, b.p. 130°C/5 mm Hg. IR (liquid film): $\nu=1690\,\mathrm{cm}^{-1}$ (aldehyde carbonyl). ^{1}H NMR; (CDCl$_3$, δ): 1·7–2·2 (4H, m); 3·2–3·4 (2H, t); 4·0–4·2 (2H, t); 6·8–7·0 (2H, d); 7·6–7·8 (2H, d); 9·8 (1H, s).

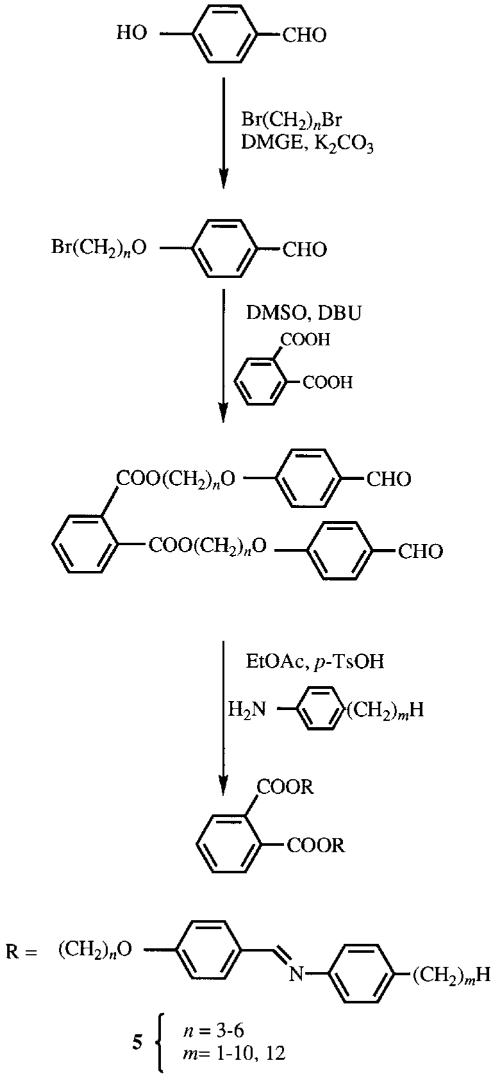

2.2. *Synthesis of benzene-1,2-di-(4-ω-carboxybutyloxybenzaldehyde)*

1,8-Diazabicyclo[5.4.0]undec-7-ene (2 eq., 0·082 mol) was added to phthalic acid (1 eq., 0·041 mol) dissolved in dry dimethyl sulphoxide (75 ml) at 40°C. After stirring the solution for 20 min, 4-ω-bromobutyloxybenzaldehyde (2·2 eq., 0·090 mol) was added and the reaction mixture stirred for 8 h at 40°C. The solution was poured into ethyl acetate (300 ml), and the solution washed with water (4 × 100 ml) and with a 5% w/v sodium carbonate solution (5 × 75 ml). The organic phase was then dried over magnesium sulphate. The ethyl acetate was removed by rotary evaporation, and unreacted aldehyde was removed by short-path distillation. The product was purified by column chromatography (90:10, diethyl ether: light petroleum, b.p. 60–80°C). Yield 56%, m.p. 76–77°C. IR (nujol mull): $\nu = 1735\,\mathrm{cm}^{-1}$ (ester carbonyl); $\nu = 1685\,\mathrm{cm}^{-1}$ (aldehyde carbonyl). ^{1}H NMR; ($CDCl_3$, δ): 1·7–2·1 (8H, m); 3·8–4·2 (4H, t); 4·2–4·5 (4H, t); 6·8–7·0 (4H, d); 7·3–7·8 (8H, m); 9·8 (2H, s).

2.3. *Synthesis of benzene-1,2-di-(4-ω-carboxybutyloxybenzylidene-4′-n-heptylaniline)* (**4,7-*ortho***)

Benzene-1,2-di-(4-ω-carboxybutyloxybenzaldehyde) (1 eq., $1{\cdot}93 \times 10^{-3}$ mol) was dissolved in dry ethyl acetate (20 ml). Freshly distilled 4-*n*-heptylaniline (2·2 eq., $4{\cdot}25 \times 10^{-3}$ mol) and a catalytic quantity of 4-toluenesulphonic acid were added and the solution was stirred for 4 h at room temperature. The resulting precipitate was isolated by filtration and purified by repeated recrystallisation from an ethyl acetate/ethanol mixture. Yield 64%. IR (nujol mull): $\nu = 1714\,\mathrm{cm}^{-1}$ (carbonyl); $\nu = 1621\,\mathrm{cm}^{-1}$ (Schiff's base). ^{1}H NMR; ($CDCl_3$, δ): 0·9 (6H, t); 1·2–1·4 (16H, m); 1·6 (4H, m); 2·0 (8H, m); 2·7 (4H, t); 4·1 (4H, t); 4·5 (4H, t); 7·0 (4H, d, $J = 9$ Hz); 7·2 (8H, m); 7·6 (2H, q, $J = 3$ Hz); 7·75 (2H, q, $J = 3$ Hz); 7·8 (4H, d, $J = 9$ Hz); 8·4 (2H, s). MS (Argon FAB): 865 (M^+, 86%), 296 ($C_{20}H_{26}NO^+$, 100%).

3. Results and discussion

Liquid crystal phases were studied and assigned using polarized light microscopy, differential scanning calorimetry (DSC), and X-ray diffraction. The optical microscopy studies were conducted using an Olympus BH-2 polarizing light microscope equipped with a Linkam TMS90 heating stage. The transition temperatures were recorded at $0{\cdot}2°\,\mathrm{min}^{-1}$ and the errors in the transition temperatures are estimated as ±1°C. Differential scanning calorimetry was carried out using a Perkin-Elmer DSC-7 and Intracooler 1 system calibrated with indium and zinc. Errors are estimated as ±1°C for the transition temperatures and as ±5% for the transitional enthalpies and entropies. X-ray diffraction experiments were carried out using a Guinier camera fitted with a bent quartz monochromator (R. Huber, Germany) and $\mathrm{CuK}_{\alpha 1}$ radiation ($\lambda = 0{\cdot}154$ nm). The error in the layer spacing, as determined from the first order reflections, is ±0·3 Å. For convenience the compounds discussed in this paper will be referred to as ***n,m-ortho*** where *n* is the number of carbon atoms in each central alkyl chain and *m* is the number of carbon atoms in each terminal alkyl chain.

3.1. *The **3,m-ortho** series*

The transition temperatures and entropies for the **3,*m-ortho*** series are presented in table 1. Almost all the liquid crystal phases exhibited by these materials are monotropic, the exceptions being homologues $m = 9$, 10 and 12. The melting temperatures and crystal to isotropic entropies show no obvious trends with respect to variations in the terminal chain length. The dependence of the liquid crystal transition temperatures on the terminal chain length for this series is plotted in figure 1. Only one compound, **3,2-*ortho***, is non-mesogenic. The compounds **3,1-*ortho*** and **3,3-*ortho*** are purely nematogenic exhibiting characteristic highly mobile, optical schlieren textures. Compounds **3,4-** and **3,5-*ortho*** exhibit smectic phases in addition to nematic phases. The magnitudes of the entropies for the nematic–isotropic transition are of the order of those found for low molar mass liquid crystals with $\Delta S/R = 0{\cdot}13$–$0{\cdot}45$; the small entropy change for this transition may be a consequence of the high molecular biaxality. The mesomorphic behaviour of compound **3,4-*ortho*** is different from that of the other

Table 1. Temperatures and entropies of transition for the **3,*m-ortho*** series; ( ) denotes a monotropic transition and ¶ denotes a transition temperature obtained by optical microscopy.

	$Cr–S_A$†, Cr–I		$S_{F/I}–S_B$†, $S_{F/I}–S_C$		$S_B–S_A$†, $S_C–S_A$		S_A–N		N–I, S_A–I†	
m	$T/°C$	$\Delta S/R$	$T/°C$	$\Delta S/R$	$T/°C$	$\Delta S/R$	$T/°C$	$\Delta S/R$	$T/°C$	$\Delta S/R$
1	106	15·79							(47)	0·13
2	118	13·27								
3	112	20·00							(66)¶	
4	100	18·76	(38)†	0·03†	(58)†	1·43	(64)	2·03	(67)	0·13
5	100	12·77	(56)	1·13	(57)		(76)	1·49	(83)	0·43
6	105	13·99	(60)	1·52	(65)				(86)†	2·86†
7	110	15·73	(68)	1·49	(73)				(99)†	3·59†
8	111	16·22	(72)	1·96	(78)				(105)†	3·72†
9	112	16·87	(78)	2·33	(82)				113†	3·93†
10	110†	13·00†	(81)	2·77	(85)				116†	3·84†
12	108†	14·05†	(87)	3·70	(92)				122†	3·47†

A further transition $X–S_{F/I}$ was noted by DSC for **3,12-*ortho*** at 29°C, $\Delta S/R = 0{\cdot}98$.

† denotes transition temperatures for the transition identified in the top row, e.g. for $m = 12$ there is a $Cr–S_A$ transition at 108°C with a $\Delta S/R$ of 14·05, and an S_A–I at 122°C.

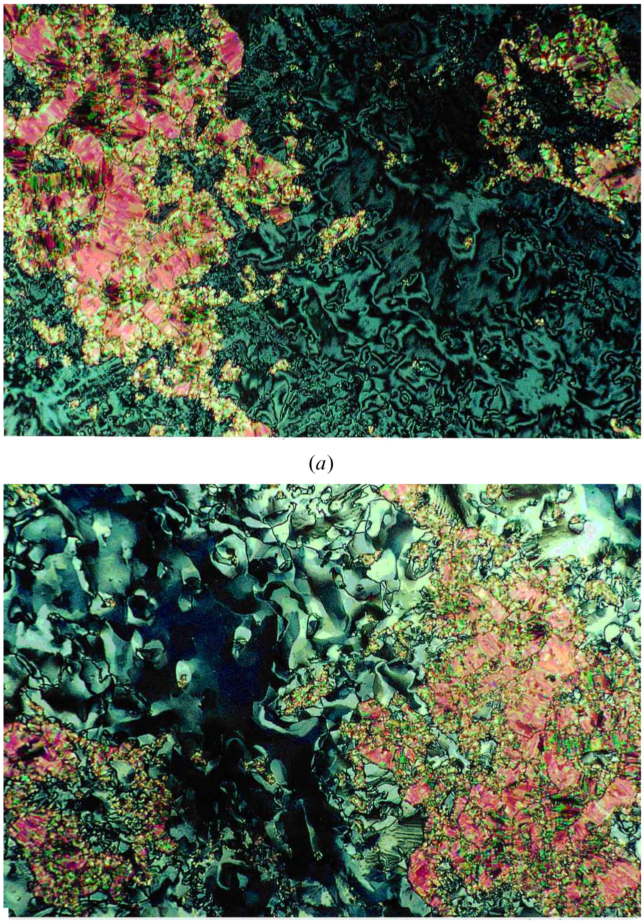

(*a*)

(*b*)

Figure 1. Optical textures of (*a*) the smectic C phase at 62°C and (*b*) the smectic F/I phase at 58°C for **4,7-*ortho***. Magnification ×120.

homologues. On cooling the nematic phase a smectic A phase forms, identifiable by its focal-conic and homeotropic textures. At lower temperatures this is followed by a smectic B phase, which is also identified by its focal-conic and homeotropic textures. The focal-conic fans differ in appearance in these two phases; those for the smectic A show some striations whilst those for the smectic B are smooth. Additionally, transition bars across the backs of the fans are observed at the transition. A smectic F/I phase forms on further cooling; the focal-conic fans of the smectic B become somewhat broken at the transition and a grey mosaic texture forms from the previously homeotropic regions. The mesogen **3,5-*ortho*** exhibits the same phase sequence as all the higher homologues, that is smectic A, smectic C and smectic F/I. The smectic C phases are identified by their focal-conic and schlieren textures, whilst the smectic F/I phases are assigned on the basis of the broken focal-conic and schlieren–mosaic textures (typical examples are shown in figure 1 for **4,7-*ortho***). The optical textures observed for the smectic F/I phases in these ***n,m-ortho*** materials are similar to those reported for the smectic F phases of the α,ω-bis(4-*n*-alkylanilinebenzylidene-4′-oxy)alkanes (***m*.O*n*O.*m*s**) [9]. Further support for the phase assignment comes from X-ray diffraction studies of the smectic F/I phase of **6,12-*ortho*** which show the phase to be hexatic. However since these data were obtained from an unaligned sample it is not possible to distinguish between smectic F and I phases. At 29°C compound **3,12-*ortho*** displays a first order transition to an unidentified phase as evidenced by DSC; however no changes in the optical textures could be noted for this transition.

It can readily be seen from figure 2 that all the phase transition temperatures increase with increasing terminal chain length. Since the molecules are U-shaped, increasing the terminal chain length is anticipated to increase significantly the length-to-breadth ratio resulting in liquid crystal phases, and particularly smectic phases, being stabilized at higher temperatures for higher homologues. The smectic A–isotropic transition entropies are of the order of magnitude of those observed for Schiff's base dimeric liquid crystals ($\Delta S/R = 2{\cdot}8$–$3{\cdot}9$) [9] and higher than those generally observed for monomeric liquid crystals ($\Delta S/R < 1{\cdot}5$) [11, 12]. These relatively high values may be a consequence of the high molecular

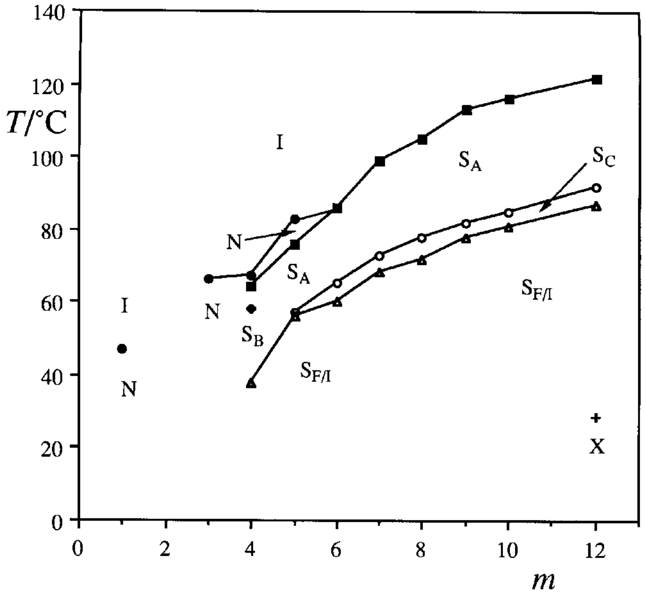

Figure 2. The dependence of the transition temperatures on the number of carbon atoms, *m*, in the terminal chains for the **3,*m*-*ortho*** series. Nematic–isotropic transitions are denoted by ●, ■ indicate smectic A–nematic or isotropic transitions, ◆ smectic B–smectic A transitions, ○ smectic C–smectic A transitions, △ smectic F/I–smectic C or smectic B transitions and +*X*–smectic F/I transitions.

weights of these materials rather than indicating a high degree of molecular ordering within the phase. However, it is interesting to note that the nematic–isotropic transition entropies are of the order of those found for monomers and lower than those for dimers. The smectic C–smectic A transitions are all second order and are characterized by a distinct step in the baseline of the DSC trace. The smectic F/I–smectic C transitions are all first order ($\Delta S/R = 1{\cdot}13$–$3{\cdot}70$) with the greater entropy changes occurring for the higher homologues. In contrast, the smectic F/I–smectic B transition for **3,4-*ortho*** is almost second order ($\Delta S/R = 0{\cdot}03$). This is not surprising as it is only the average tilt angle of the molecules with respect to the director that distinguishes these two phases.

X-ray diffractograms obtained from the smectic A phase formed by compound **3,7-*ortho*** give a layer spacing of $d = 53{\cdot}4 \pm 0{\cdot}3$ Å, whereas the length of the molecule (l), with its alkyl chains in the all-*trans*-conformation, was estimated to be ≈31 Å from a computer generated model. The ratio $d/l \approx 1{\cdot}72$ suggests that in this smectic A phase the molecules are ordered into bilayers. The significance of this result will be discussed in §3·5. It should be noted that the X-ray diffractogram exhibits two orders of reflection in the small angle region indicating a high degree of molecular ordering in the smectic A phase. The large entropy change ($\Delta S/R = 3{\cdot}59$) measured for the S_A–I transition of this compound is consistent with this inference.

3.2. *The **4,m-ortho** series*

The temperatures and entropies of transition for the **4,*m*-*ortho*** series are given in table 2. In common with the **3,*m*-*ortho*** series, the majority of the liquid crystal phases are monotropic and the melting points show no obvious trends with respect to the length of the terminal chain. The crystal–smectic C transition entropies are high ($\Delta S/R > 25$). The most striking feature of this series is the absence of nematic phases. All the compounds form smectic phases and interestingly the first three homologues form smectic B phases. Compounds **4,1-** and **4,2-*ortho*** form smectic B phases exclusively, whilst **4,3-*ortho*** also exhibits a smectic A phase with a 3°C range as a higher temperature modification. All subsequent homologues form the smectic A phase. The entropy changes for the smectic B–isotropic transition are high, $\Delta S/R \sim 5$, a consequence of the high degree of molecular ordering in this hexatic phase. In contrast, the smectic A–isotropic transition entropy for **4,3-*ortho*** is 2·58. On increasing the terminal chain length, the S_A–I transitional entropies increase to $\Delta S/R = 4{\cdot}9$ for the **4,12-*ortho*** homologue.

The transition temperature dependence on terminal chain length for the **4,*m*-*ortho*** series is shown in figure 3. The increase in stability of the smectic A, smectic C and smectic F/I phases on increasing m is apparent. Indeed, the clearing temperature is almost stable for the first four homologues and then increases steadily from 56°C for **4,4-*ortho*** to 111°C for **4,12-*ortho***. The increase in clearing temperature for these homologues is similar to that observed for the **3,*m*-** series. In common with the **3,*m*-*ortho*** series the $m = 4$ homologue in the **4,*m*-*ortho*** series exhibits a phase sequence that is unique. In this case the transition to the smectic F/I phase occurs directly from the smectic A phase rather than via a smectic C phase. The entropy change for the $S_{F/I}$–S_A transition is $\Delta S/R = 0{\cdot}79$ whilst for the $S_{F/I}$–S_C transitions this ranges from 0·67 for **4,5-*ortho*** to 3·13 for **4,12-*ortho***. The focal-conic fans in the smectic C phase are somewhat broken and sanded; on forming the smectic F/I phase these breakages become more prominent but do not transform into the black patches that are often reported

Table 2. Temperatures and entropies of transition for the **4,*m*-*ortho*** series; ( ) denotes a monotropic transition.

	Cr–S_A†, Cr–S_C¶, Cr–I		$S_{F/I}$–S_A, $S_{F/I}$–S_C		S_B–S_A†, S_C–S_A		S_B–I†, S_A–I	
m	T/°C	$\Delta S/R$	T/°C	$\Delta S/R$	T/°C	$\Delta S/R$	T/°C	$\Delta S/R$
1	105	17·80					(60)†	5·25†
2	96	15·04					(60)†	5·03†
3	84	19·93			(56)†	1·35†	(59)	2·58
4	86	17·85	(50)†	0·79†			(56)	2·56
5	85	18·32	(46)	0·67	(47)		(66)	2·66
6	84	19·02	(52)	0·84	(59)		(73)	3·56
7	96	17·65	(60)	0·96	(66)		(88)	4·22
8	82	21·20	(65)	1·06	(74)		94	4·10
9	94†	21·69†	(72)	1·76	(79)		102	4·84
10	81¶	25·33¶	(75)	2·05	83		105	4·81
12	89¶	29·58¶	(83)	3·13	91		111	4·91

A further transition X–$S_{F/I}$ was noted by DSC for **4,12-*ortho*** at 28°C, $\Delta S/R = 1{\cdot}18$.

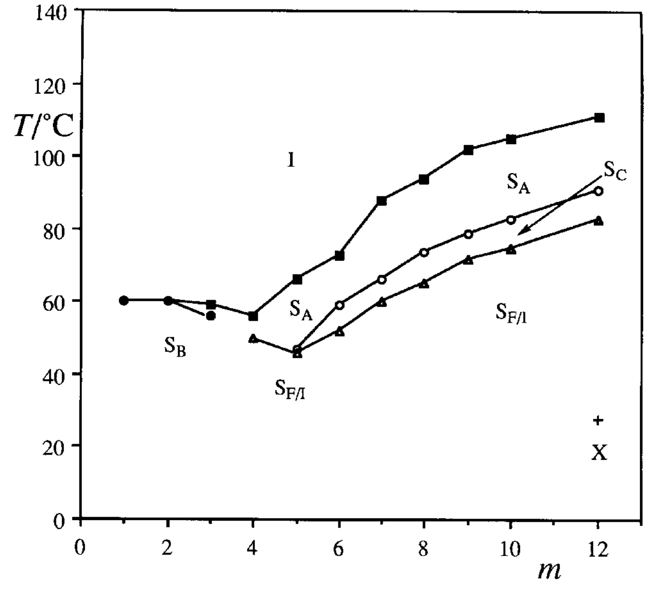

Figure 3. The dependence of the transition temperatures on the number of carbon atoms, *m*, in the terminal chains for the **4,*m*-*ortho*** series. Smectic B–isotropic or smectic A transitions are denoted by ●, ■ indicate smectic A–isotropic transitions, ○ smectic C–smectic A transitions, △ smectic F/I–smectic C transitions and + *X*–smectic F/I transitions.

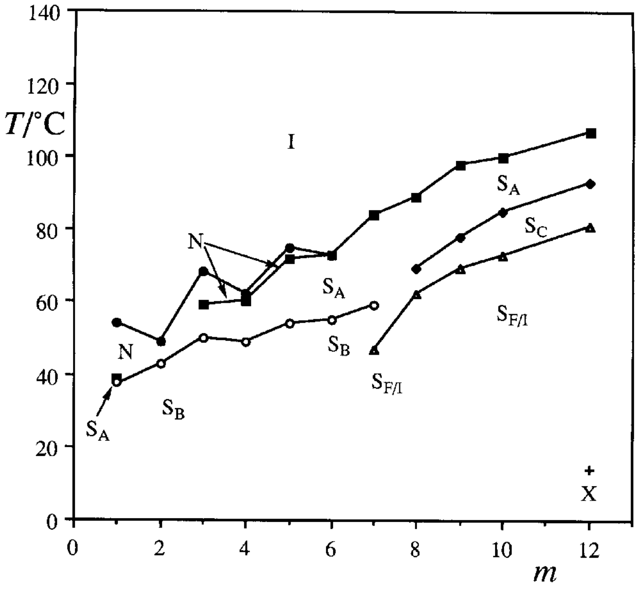

Figure 4. The dependence of the transition temperatures on the number of carbon atoms, *m*, in the terminal chains for the **5,*m*-*ortho*** series. Nematic–isotropic transitions are denoted by ●, ■ indicate smectic A–nematic or isotropic transitions, ○ smectic B–smectic A or nematic transitions, ◆ smectic C–smectic A transitions, △ smectic F/I–smectic C or smectic B transitions and + *X*–smectic F/I transitions.

for a smectic F or I phase [13]. Compound **4,12-*ortho*** also exhibits a first order transition to an unidentified phase at 28°C.

3.3. *The* ***5,m-ortho*** *series*

The transition entropies and temperatures for the **5,*m*-*ortho*** series are given in table 3. All the compounds are mesomorphic; however only the smectic A phases for **5,10-** and **5,12-*ortho*** are enantiotropic. The dependence of the phase transition temperatures on terminal chain length is plotted in figure 4. The first five members of the series form nematic phases. An odd–even alternation of the N–I transition temperatures can be seen for these homologues, with compounds having an odd number of carbon atoms in the terminal chain exhibiting the higher transition temperatures. The transition entropies exhibit an analogous parity dependence. These observations are in accord with those for low molar mass liquid crystals [14]. Members of the series with $m > 5$ are purely

Table 3. Temperatures and entropies of transition for the **5,*m*-*ortho*** series; § denotes overlapping peaks and ( ) a monotropic transition.

	Cr–S_A†, Cr–I		$S_{F/I}$–S_C, $S_{F/I}$–S_B†		S_B–S_A†, S_C–S_A		S_B–N†, S_A–N		N–I, S_A–I†	
m	*T*/°C	$\Delta S/R$	*T*/°C	$\Delta S/R$	*T*/°C	$\Delta S/R$	*T*/°C	$\Delta S/R$	*T*/°C	$\Delta S/R$
1	105	22·67			(38)†	§	(39)	§	(54)	0·32
2	96	14·81					(43)†	3·80†	(49)	0·14
3	94	15·24			(50)†	1·49†	(59)	1·52	(68)	0·38
4	83	20·77			(49)†	1·21†	(60)	1·92	(62)	0·25
5	82	17·52			(54)†	1·36†	(72)	1·77	(75)	0·47
6	98	18·66			(55)†	1·20†			(73)†	2·98†
7	104	20·77	(47)†		(59)†	1·23†			(84)†	3·95†
8	103	19·59	(62)	1·32	(69)				(89)†	4·47†
9	104	20·46	(69)	1·68	(78)				(98)†	5·03†
10	100	20·28	(73)	1·99	(85)				100†	5·20†
12	99†	16·19†	(81)	2·78	(93)				107†	5·55†

A further transition X–$S_{F/I}$ was noted by DSC for **5,12-*ortho*** at 14°C, $\Delta S/R = 2{\cdot}50$.

smectogenic with smectic A phases occurring as the high temperature modification. The smectic A–isotropic transition temperatures also appear to exhibit an odd–even alternation in transition temperatures, although its magnitude is less than that for the nematic–isotropic transitions. The S_A–I transition entropies increase with increasing *m*, reaching a maximal value of $\Delta S/R=5{\cdot}5$, but do not appear to alternate. With the exception of **5,2-*ortho*** all members of this series form a smectic A phase. The first seven homologues all form smectic B phases and the remaining homologues exhibit smectic C and smectic F/I phases. The entropy changes for the $S_{F/I}$–S_C transition increase from $\Delta S/R=1{\cdot}32$ for **5,8-*ortho*** to $\Delta S/R=2{\cdot}78$ for **5,12-*ortho***. Compound **5,7-*ortho*** forms the smectic F/I phase from the smectic B and this transition is second order. DSC studies show that compound **5,12-*ortho*** undergoes a further first order transition to an unidentified phase at 14°C.

3.4. *The* ***6,m-ortho*** *series*

The temperatures and entropies of transition for the **6,*m*-*ortho*** series are presented in table 4. In common with the other ***n,m-ortho*** series described so far, the majority of the liquid crystal phases are monotropic, with the melting points showing no obvious trends with respect to the terminal chain length. As in the case of the **4,*m*-*ortho*** series, the most striking feature of this series is the absence of nematic phases. All the compounds form smectic phases and the first seven homologues form smectic B phases, the transition temperatures for which show little or no dependence on the terminal chain length. For **6,1-** and **6,2-*ortho*** the smectic B phase is the only mesophase exhibited. All other homologues form smectic A phases. The dependence of the phase transition temperatures on terminal chain length is plotted in figure 5. The clearing temperatures appear to show an odd–even alternation as a function of the parity of the terminal chain. The clearing entropies show this trend only for the early members ($m=3$–6) of the series. The transition temperatures for the smectic A, smectic C and smectic F/I phases that occur when $m>7$ increase with increasing terminal chain length, as do the clearing and $S_{F/I}$–S_C transitional entropies. Compound **6,12-*ortho*** exhibits a first order transition at 18°C (by DSC) for which no changes in the optical textures could be seen.

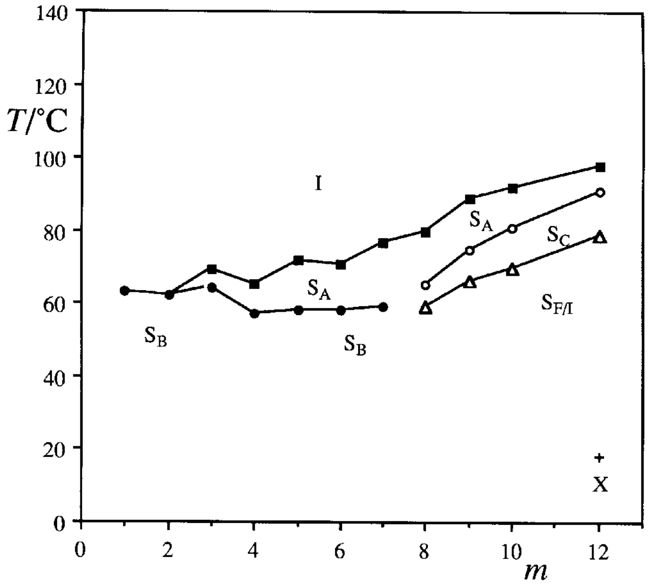

Figure 5. The dependence of the transition temperatures on the number of carbon atoms, *m*, in the terminal chains for the **6,*m*-*ortho*** series. Smectic B–isotropic or smectic A transitions are denoted by ●, ■ indicate smectic A–isotropic transitions, ○ smectic C–smectic A transitions, △ smectic F/I–smectic C transitions and $+X$–smectic F/I transitions.

Table 4. Temperatures and entropies of transition for the **6,*m*-*ortho*** series; ( ) denotes a monotropic transition.

	Cr–S_A†, Cr–S_C¶, Cr–I		$S_{F/I}$–S_C		S_B–S_A†, S_C–S_A		S_B–I†, S_A–I	
m	*T*/°C	Δ*S*/*R*	*T*/°C	Δ*S*/*R*	*T*/°C	Δ*S*/*R*	*T*/°C	Δ*S*/*R*
1	123	24·85					(63)†	5·78†
2	87	23·00					(62)†	6·05†
3	85	21·55			(64)†	1·77†	(69)	3·37
4	81	24·20			(57)†	1·64†	(65)	3·54
5	75	20·78			(57)†	1·48†	(72)	3·35
6	76	22·26			(58)†	1·46†	(71)	3·58
7	82	19·67			(59)†	1·42†	(77)	3·96
8	79	25·99	(59)	1·27	(65)		80	4·82
9	77	16·59	(66)	1·51	(75)		89	5·50
10	82†	13·49†	(70)	1·90	81		92	5·81
12	80¶	32·82¶	(79)	2·60	91		98	6·40

A further transition X–$S_{F/I}$ was noted by DSC for **6,12-*ortho*** at 18°C, $\Delta S/R=4{\cdot}50$.

Compound **6,12-*ortho*** was studied by X-ray diffraction. The diffraction pattern for the smectic A phase of this material exhibits two orders of reflection at small angle. The entropy change for the smectic A–isotropic transition was found to be $\Delta S/R = 6{\cdot}40$. Both these results suggest that the molecules are highly ordered in the smectic A phase. The assignment of the smectic F/I phase in this series is confirmed by the sharpening of the wide angle diffraction at the transition from the smectic C phase. This indicates that the molecular ordering is no longer liquid-like within the layers. The wide angle scattering has only one maximum in the intensity indicating that a crystal phase has not formed. In the smectic A phase of this compound ($T = 96°$C), the layer spacing was found to be $69{\cdot}9 \pm 0{\cdot}3$ Å. The molecular length estimated from a molecular model is 38 Å. The layer spacings of the smectic C and smectic F/I phases were $68{\cdot}9 \pm 0{\cdot}3$ Å (at 81°C) and $74{\cdot}3 \pm 0{\cdot}3$ Å (at 75°C) respectively. Thus in the smectic phases of the **6,12-*ortho*** compound the molecules appear to be arranged in bilayers. The formation of a bilayer hexatic phase is most unusual and, to our knowledge, has been reported only in the case of the smectic B phase for a series of 4-cyanoalkoxybenzylidene-4′-alkylanilines [15].

4. General observations

There are a number of striking similarities in the mesomorphic behaviour of the four ***n,m-ortho*** homologous series. In figure 6 the clearing temperatures of the four series are plotted against the length (m) of the terminal chain. As can be seen from figure 6 (*a*), the odd spacer compounds ($n = 3,5$) form nematic phases for $m < 6$, and smectic A phases otherwise as the high temperature modification. In contrast, the compounds with even spacer chains ($n = 4,6$) have smectic B–isotropic transitions for the first two homologues and smectic A–isotropic transitions otherwise. Thus the parity of the spacer plays an important role in determining the liquid crystal polymorphism at short terminal chain lengths. For long terminal chain lengths all the homologous series exhibit an identical mesophase sequence, namely, $S_{F/I}$–S_C–S_A–I. The clearing temperatures at short terminal chain lengths are lower for the $n = 3$ and $n = 5$ compounds when compared with the $n = 4$ and $n = 6$ materials respectively (see figure 6). However this trend is reversed at higher terminal chain lengths.

On comparing the entropy changes for the clearing transitions (figure 7), it is interesting to note that those for the **3,*m-ortho*** series rise to a limiting value ($\Delta S/R = 3{\cdot}93$ for $m = 9$), whereas those for the **5,*m-ortho*** go through a maximum. In contrast, entropy changes for the **4,*m-ortho*** series increase and then stabilize with increasing terminal chain length, while those for the **6,*m-ortho*** series continue to increase with increasing m. This rise in transitional entropies is such that in the latter two series the S_A–I entropy changes for higher homologues are comparable with the S_B–I transitional entropies for the early homologues (figure 7 (*b*)).

Comparison of the series shows that increasing the spacer chain length promotes the formation of smectic B phases. For the **3,*m*-**, **4,*m*-**, **5,*m*-**, and **6,*m*-** series one, three, seven, and seven homologues, respectively, form smectic B phases. All four compounds having $m = 12$ exhibit a first order transition to an unidentified phase at low temperatures (10–30°C).

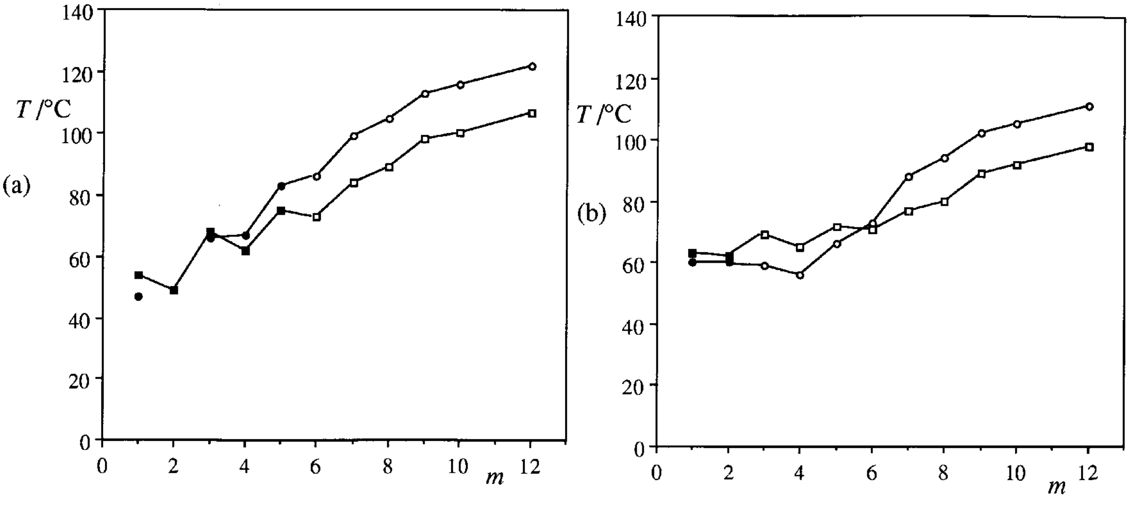

Figure 6. Comparison of clearing point transitions for the ***n,m-ortho*** series. (*a*) ●, ■ denote nematic–isotropic transitions and ○, □ indicate smectic A–isotropic transitions for the **3,*m-ortho*** and **5,*m-ortho*** series, respectively. (*b*) ●, ■ denote smectic B–isotropic transitions and ○, □ indicate smectic A–isotropic transitions for the **4,*m-ortho*** and **6,*m-ortho*** series, respectively.

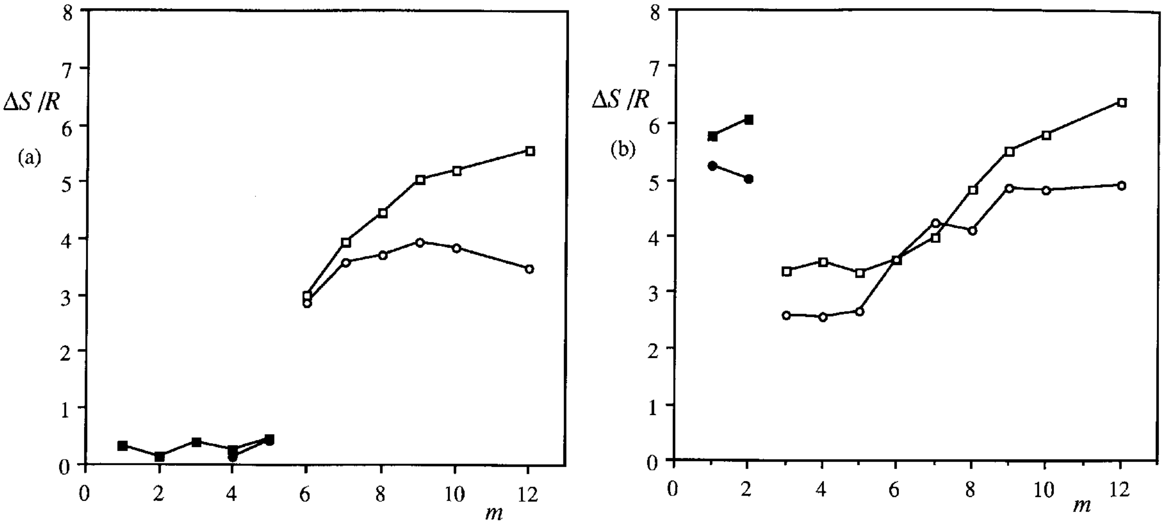

Figure 7. Comparison of the entropies of transition for the ***n,m*-ortho** series. (*a*) ●, ■ denote nematic–isotropic transitions and ○, □ indicate smectic A–isotropic transitions for the **3,*m*-ortho** and **5,*m*-ortho** series, respectively. (*b*) ●, ■ denote smectic B–isotropic transitions and ○, □ indicate smectic A–isotropic transitions for the **4,*m*-ortho** and **6,*m*-ortho** series, respectively.

In order to evaluate the effect of spacer chain length on the liquid crystal properties, the smectic A–isotropic transition temperatures as a function of *n* are plotted in figure 8 (*a*) which shows that transition temperatures fall with increasing *n*. The dependence of the smectic A–isotropic transition entropy on *n* is plotted in figure 8 (*b*). In contrast to the transition temperatures, the entropies increase with increasing spacer chain length for $m>7$. These increases are quite considerable; for example for $m=12$, $\Delta S/R$ increases from 3·47 for the compound having $n=3$ to 6·40 for the compound with $n=6$. Increasing the spacer length affords greater conformational freedom that could allow the rod-like moieties to align more efficiently with respect to the director and so pack more efficiently in the mesophase. This increase in the molecular ordering of the mesophase increases the entropy change at the transition to the isotropic phase.

It has already been noted that in the $n=4$ and 6 series the molecules are unable to form nematic phases regardless of terminal chain length. Initial members exhibit smectic B–isotropic transitions which give way to smectic A–isotropic transitions on increasing *m*. Such behaviour is uncommon. In contrast, for the $n=3,5$ homologous series, the dependence of the mesomorphic behaviour on length of the terminal chain is similar to

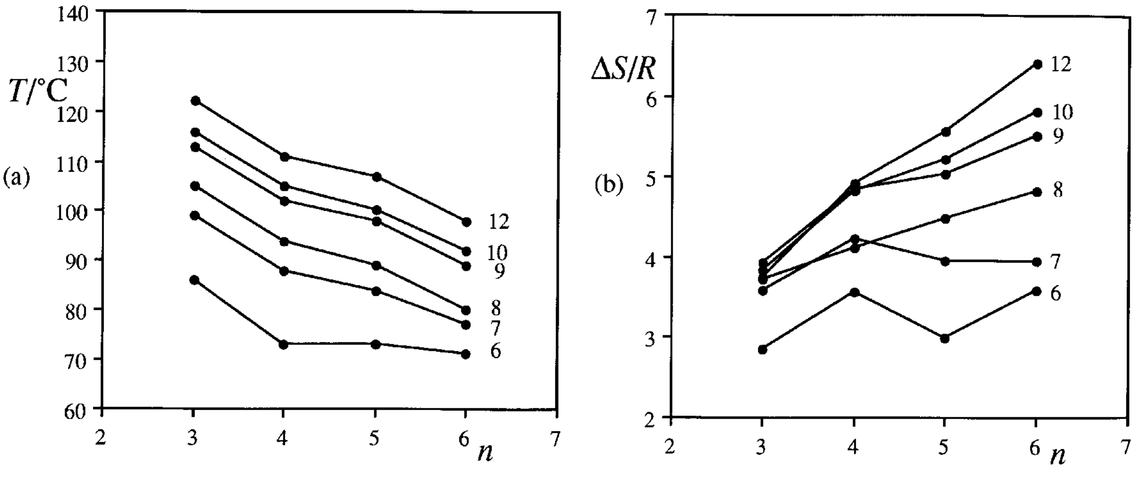

Figure 8. Dependence of the smectic A–isotropic (*a*) transition temperatures and (*b*) transitional entropy changes on spacer chain length, *n*, for the ***n,m*-ortho** compounds. The numbers on the graphs indicate the terminal chain lengths, *m*.

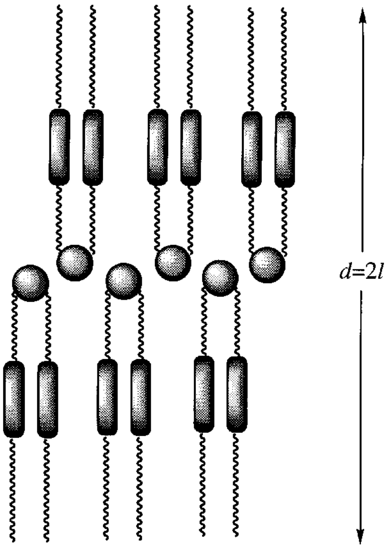

Figure 9. Schematic of possible molecular packing in the bilayer smectic phases for the ***n,m-ortho*** compounds.

that found for monomeric liquid crystals [14]. Nematic phases form for early members of the series and the nematic–isotropic transition temperatures and entropy changes exhibit a parity dependence. Smectic phase stability increases with increasing terminal chain length to the extent that for higher homologues no nematic phases are observed. Indeed tilted phases are preferentially formed by homologues with long terminal chains. The mesomorphic properties of the long chain homologues of the $n=4,6$ series are similar to those of the $n=3,5$ series. X-ray diffraction studies have shown that in the smectic A phases of the **3,7-*ortho*** and the **6,12-*ortho*** compounds the molecules are arranged in bilayers (figure 9). This behaviour is similar to that of 1,2-disubstituted compounds with Schiff's bases directly attached to the core where partial bilayer smectic phases have been reported [4, 5].

We thank A. E. Blatch (Southampton University) and J. M. Seddon (Imperial College) for providing the X-ray pictures and acknowledge the EPSRC for the award of a studentship to A. G. Douglass.

References

[1] Vorländer, D., 1907, *Chem. Ber.*, **40,** 1970.

[2] Demus, D., 1989, *Liq. Cryst.*, **5,** 75.

[3] Vorländer, D., and Apel, A., 1932, *Chem. Ber.*, **65,** 1101.

[4] Kuboshita, M., Matsunaga, Y., and Matsuzaki, H., 1991, *Mol. Cryst. Liq. Cryst.*, **199,** 319.

[5] Matsunaga, Y., and Matsuzaki, H., 1993, *Liq. Cryst.*, **14,** 105.

[6] Kato, T., Adachi, H., Fujishima, A., and Fréchet, J. M. J., 1992, *Chem. Lett.*, 265.

[7] Griffin, A. C., and Britt, T. R., 1981, *J. Am. chem. Soc.*, **103,** 4957.

[8] Emsley, J. W., Luckhurst, G. R., Shilstone, G. N., and Sage, I., 1984, *Mol. Cryst. Liq. Cryst.*, **102,** 223.

[9] Date, R. W., Imrie, C. T., Luckhurst, G. R., and Seddon, J. W., 1992, *Liq. Cryst.*, **12,** 203.

[10] Nishikubo, T., Iizawa, T., Takahashi, A., and Shimokawa, T., 1990, *J. Polym. Sci. A; Polym. Chem.*, **28,** 105.

[11] Keller, P., and Liebert, L., 1978, *Solid State Phys. Suppl.*, **14,** 19.

[12] Smith, G. W., and Garland, Z. G., 1973, *J. chem. Phys.*, **59,** 3214.

[13] Gray, G. W., and Goodby, J. W., 1984, *Smectic Liquid Crystals* (Leonard Hill).

[14] Gray, G. W., 1979, *The Molecular Physics of Liquid Crystals*, edited by G.R. Luckhurst and G.W. Gray (Academic Press), Chaps. 1, 12.

[15] Barbarin, F., Dugay, M., Piovesan, A., Fadel, H., Guillon, D., and Skoulios, A., 1987, *Liq. Cryst.*, **2,** 815.